Microwave Complex Conductivity of a Square Post in Rectangular Waveguide

SHINZO YOSHIKADO AND ICHIRO TANIGUCHI

Abstract—**A simple measurement technique for the complex conductivity of a square lossy dielectric post loaded in a rectangular waveguide is described. The measurement technique is based on a solution of the reflection coefficient for the incident electric field of the TE_{10} mode. The reflection coefficient can be expressed by a simple formula for the electric fields scattered from the post. Values of complex conductivities of standard materials were calculated by applying an iteration method to this formula with respect to measured values of reflection coefficients. These agreed with the values measured by other techniques and reported by several authors. The present method is also applicable to measurements related to filling the cross section of the waveguide with a dielectric material.**

I. Introduction

VARIOUS theories and techniques for determining the microwave complex conductivity of a post of dielectric material, semiconductor, plasma, etc., in a rectangular waveguide have been proposed [1]–[11]. The method using posts instead of the usual method of filling the cross section of the waveguide offers the advantage of being able to measure any complex conductivity of a small amount of material. Each investigator has employed a method adequate for the size and the shape of a particular post. It is difficult to obtain the complex conductivity of a dielectric post with a cross section of arbitrary shape [9]–[11]. A number of authors have dealt with a circular post by approximate analytical methods or numerical methods [1]–[11].

We are interested in ionic conduction in single crystals of one-dimensional superionic conductor priderites with hollandite-type structure [12]. Single crystals of priderites grow well in the direction of a c axis with a square cross section and have various cross-sectional sizes. Furthermore, their complex conductivity along the c axis is large. It is difficult to process such materials into a cylindrical shape. However, neither an analytical nor a numerical solution for a square post has ever been proposed. This is due to the difficulty of obtaining rigorous solutions for the reflection and transmission coefficient, because the Helmholtz partial differential equation for the electromagnetic fields must be solved under inhomogeneous boundary conditions at the surface of a post, as in the case of a circular post.

Holms *et al.* measured the microwave conductivity of thin circular posts of silicon and germanium using the transmission line equivalent circuit [2]. Their equivalent circuit method is applicable to a circular post having a diameter less than ~ 0.24 cm and a conductivity less than ~ 0.1 S/cm for a dielectric constant of about 16 at X-band. They also showed that the reflection or transmission coefficient for thin circular posts was equal to those for square posts with equivalent area. However, this might not be true for a thicker or an oblong post.

The first purpose of this study is to derive an approximate analytical solution for the Helmholtz equation for a square post by introducing the discrete boundary conditions. The second purpose is to establish a simple method for measuring the complex conductivity of a square lossy dielectric post. The validity of the solution for the complex conductivities was verified by laboratory measurements at X-band for posts of PTFE (polytetrafluoroethylene), synthetic quartz glass, sintered alumina ceramics (Al_2O_3), rutile (TiO_2), and germanium (Ge). The complex conductivities of these materials are known from the literature or from other measurement techniques. Numerical estimation of the measurement error arising from positioning error is carried out. A comparison between the method using posts and the usual method of completely filling the cross section of the waveguide is made. The c axis complex conductivity of a single crystal of priderite, $K_{1.6}Mg_{0.8}Ti_{7.2}O_{16}$, was measured by the present method and the results are shown.

II. Basic Formulation

A. Scattered Field in a Rectangular Waveguide Loaded with a Square Post

A waveguide loaded with a square post is shown in Fig. 1. The axis of the post is parallel to the y axis of the waveguide. As the TE_{10} mode is assumed incident on the post from the region $z < 0$, as shown in Fig. 2, the electric field in the post has only a y component, $E_{int}(x, z)$. With the assumption of harmonic variation of the field and with a time factor $\exp(i\omega t)$, the wave equation satisfied by the internal electric field E_{int} is

$$\left(\frac{\partial^2}{\partial x^2} + \frac{\partial^2}{\partial z^2} - i\omega\mu_0\dot{\sigma}\right) E_{int} = 0 \tag{1}$$

where μ_0 is the permeability of free space, and $\dot{\sigma}$ is the complex conductivity parallel to a y axis [13], [14]. The quantity $\dot{\sigma}$ is related to both the conductivity σ and the dielectric constant ϵ as $\dot{\sigma} = \sigma + i\omega\epsilon_0\epsilon$, where ϵ_0 is the

Manuscript received November 12, 1987; revised January 20, 1988.
The authors are with the Department of Electronics, Doshisha University, Kyoto 602, Japan.
IEEE Log Number 8927163.

0018-9480/89/0600-0984$01.00

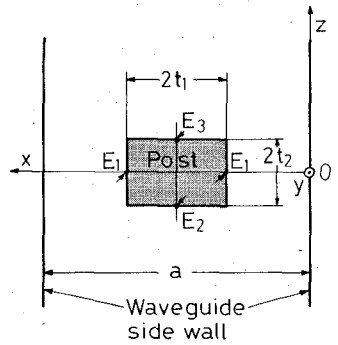

Fig. 1. A waveguide loaded with a square post parallel to the y axis.

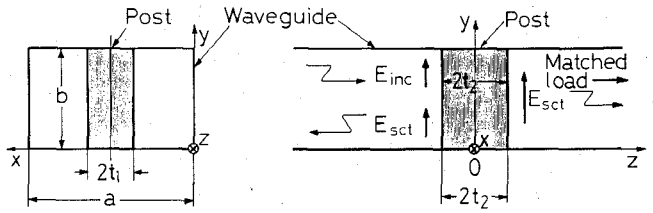

Fig. 2. The cross section and the longitudinal section of a waveguide loaded with a post. The TE_{10} mode is assumed incident on the post from the region $z<0$. E_{inc} is the incident electric field of the TE_{10} mode. E_{sct} is the scattered electric field from the post.

permittivity of free space. It is difficult to obtain the complete form of the exact Green's function for the inhomogeneous boundary conditions for (1). Giving the following discrete boundary conditions to E_{int} at the surface of the post:

$$E_{int}(a/2\pm t_1,0)=E_1 \tag{2}$$

$$E_{int}(a/2,-t_2)=E_3 \tag{3}$$

$$E_{int}(a/2,t_2)=E_2 \tag{4}$$

the approximate solution of (1) is

$$E_{int}=\left[\frac{E_1}{\cosh c_1t_1}\cosh c_2z+\frac{E_2-E_3}{2\sinh c_2t_2}\sinh c_2z\right]\cdot\cosh c_1\left(x-\frac{a}{2}\right) \tag{5}$$

where $c_1^2+c_2^2=i\omega\mu_0\dot{\sigma}$. In this case, the complete form of the exact Green's function for the inhomogeneous boundary conditions for (1) is not obtained.

The scattered electric field from the post has only a y component, $E_{sct}(x,z)$. The wave equation satisfied by E_{sct} is

$$\left(\frac{\partial^2}{\partial x^2}+\frac{\partial^2}{\partial z^2}+k_0^2\right)E_{sct}=i\omega\mu_0\dot{\sigma}_nE_{int}\left(H\left(x-\frac{a}{2}+t_1\right)-H\left(x-\frac{a}{2}-t_1\right)\right)(H(z+t_2)-H(z-t_2)) \tag{6}$$

where $k_0=2\pi/\lambda$ (λ being the wavelength in free space), $\dot{\sigma}_n=\dot{\sigma}-i\omega\epsilon_0$, and $H(\ )$ is the Heaviside function [13], [14]. The modes with odd number, $TE_{2n-1\,0}$ modes, are excited by the post, because it is symmetrically loaded in the waveguide. The solutions of (6) are given by

$$E_{sct}=\frac{2}{a}\sum_{n=1}^{\infty}K_{2n-1}^{-}e^{\Gamma_{2n-1}z}\sin\frac{(2n-1)\pi x}{a},\qquad z\leqslant -t_2 \tag{7}$$

$$E_{sct}=\frac{2}{a}\sum_{n=1}^{\infty}\left(I_{2n-1}\cosh c_2z+J_{2n-1}\sinh c_2z+L_{2n-1}^{-}e^{\Gamma_{2n-1}z}+L_{2n-1}^{+}e^{-\Gamma_{2n-1}z}\right)\sin\frac{(2n-1)\pi x}{a},$$

$$0\leqslant x\leqslant a/2-t_1,\ a/2+t_1\leqslant x\leqslant a,\ -t_2\leqslant z\leqslant t_2 \tag{8}$$

$$E_{sct}=\frac{2}{a}\sum_{n=1}^{\infty}K_{2n-1}^{+}e^{-\Gamma_{2n-1}z}\sin\frac{(2n-1)\pi x}{a},\qquad z\geqslant t_2 \tag{9}$$

where $\Gamma_n^2=n^2\pi^2/a^2-k_0^2$. The boundary conditions whereby E_{sct} and $\partial E_{sct}/\partial z$ must be continuous at $z=\pm t_2$ give

$$K_{2n-1}^{\pm}=\frac{1}{\Gamma_{2n-1}}\left[(\Gamma_{2n-1}I_{2n-1}\mp c_2J_{2n-1})\cosh c_2t_2\sinh\Gamma_{2n-1}t_2-(c_2I_{2n-1}\mp\Gamma_{2n-1}J_{2n-1})\sinh c_2t_2\cosh\Gamma_{2n-1}t_2\right] \tag{10}$$

$$L_{2n-1}^{\pm}=-\frac{e^{-\Gamma_{2n-1}t_2}}{2\Gamma_{2n-1}}\left[(\Gamma_{2n-1}I_{2n-1}\mp c_2J_{2n-1})\cosh c_2t_2+(c_2I_{2n-1}\mp\Gamma_{2n-1}J_{2n-1})\sinh c_2t_2\right] \tag{11}$$

where

$$I_{2n-1}=i\omega\mu_0\dot{\sigma}_nF_{2n-1}\frac{1}{c_2^2-\Gamma_{2n-1}^2}\frac{E_1}{\cosh c_1t_1} \tag{12}$$

$$J_{2n-1}=i\omega\mu_0\dot{\sigma}_nF_{2n-1}\frac{1}{c_2^2-\Gamma_{2n-1}^2}\frac{E_2-E_3}{2\sinh c_2t_2} \tag{13}$$

$$F_{2n-1}=(-1)^{n-1}\left[\frac{1}{c_1+i(2n-1)\pi/a}\cdot\sinh\left[c_1a+i(2n-1)\pi\right]+\frac{1}{c_1-i(2n-1)\pi/a}\sinh\left[c_1a-i(2n-1)\pi\right]\right]. \tag{14}$$

The scattered electric field E_{sct} depends on both E_1 and E_2-E_3. The boundary conditions at the surface of the post are

$$E_{inc}+E_{sct}=\begin{cases}E_1, & x=\dfrac{a}{2}\pm t_1,\ z=0 \quad (15)\\ E_2, & x=\dfrac{a}{2},\ z=-t_2 \quad (16)\\ E_3, & x=\dfrac{a}{2},\ z=t_2 \quad (17)\end{cases}$$

where $E_{inc}(x,z)=E_0\sin(\pi x/a)e^{-\Gamma_1z}$ is the incident electric field. From (7)–(17), E_1 and E_2-E_3 are given by

$$E_1=E_0A \tag{18}$$

$$E_2-E_3=-E_0B \tag{19}$$

where

$$A = \cosh\Gamma_1 t_2 \frac{\cosh c_1 t_1}{\cosh c_2 t_2}\left[1 - i\omega\mu_0\dot{\sigma}_n \frac{1}{\cosh c_1 t_1}\frac{2}{a} \cdot \sum_{n=1}^{\infty} \frac{(-1)^n F_{2n-1} e^{-\Gamma_{2n-1}t_2}}{\Gamma_{2n-1}(c^2 - \Gamma_{2n-1}^2)} \cdot (\Gamma_{2n-1}\cosh c_1 t_1 \sinh\Gamma_{2n-1}t_2 - c_2 \sinh c_2 t_2 \cosh\Gamma_{2n-1}t_2)\right]^{-1} \quad (20)$$

and

$$B = 2\sinh\Gamma_1 t_2\left[1 + i\omega\mu_0\dot{\sigma}_n \frac{1}{2\sinh c_2 t_2}\frac{2}{a} \cdot \sum_{n=1}^{\infty} \frac{(-1)^n F_{2n-1} e^{-\Gamma_{2n-1}t_2}}{\Gamma_{2n-1}(c_2^2 - \Gamma_{2n-1}^2)} \cdot (c_2\cosh c_2 t_2 \sinh\Gamma_{2n-12}^{t} - \Gamma_{2n-1}\sinh c_1 t_1 \cosh\Gamma_{2n-1}t^2)\right]^{-1}. \quad (21)$$

The $R(z)$ for $z \ll -t_2$ and $T(z)$ for $z \gg t_2$, where E_{sct} has only the TE_{10} mode, are given by

$$R(z) = P^- e^{2\Gamma_1 z} = \dot{\sigma}_n P^{-\prime} e^{2\Gamma_1 z} \quad (22)$$

$$T(z) = 1 + P^+ = 1 + \dot{\sigma}_n P^{+\prime} \quad (23)$$

where

$$P^{\pm\prime} = \frac{2}{a}\frac{i\omega\mu_0 F_1}{\Gamma_1(c_2^2 - \Gamma_1^2)}\left[\left(\Gamma_1 \frac{A}{\cosh c_2 t_2} \pm c_2 \frac{B}{2\sinh c_2 t_2}\right) \cdot \cosh c_2 t_2 \sinh\Gamma_1 t_2 - \left(c_2 \frac{A}{\cosh c_2 t_2} \pm \Gamma_1 \frac{B}{2\sinh c_2 t_2}\right)\sinh c_2 t_2 \cosh\Gamma_1 t_2\right]. \quad (24)$$

If $R(z)$ or $T(z)$ is measured, the complex conductivity $\dot{\sigma}$ of a post is obtained by solving (22) or (23).

B. Measurement of Reflection Coefficient

A waveguide-matched termination method has been generally used to measure $R(z)$ or $T(z)$ [2]–[4], [7], [8]. To measure small $R(z)$ or large $T(z)$, a good waveguide-matched termination with a low voltage standing wave ratio (~ 1) must be connected to the waveguide cell. However, it is not convenient to calibrate the effect of a reflection of a small microwave signal from the termination on $R(z)$. Therefore, it is convenient to terminate the waveguide cell with a shorting plate at an appropriate position, $z = z_s$. In this case, the reflection coefficient is given by taking the multiple reflections between the post and the shorting plate into consideration. Here, the waveguide cell was terminated at $z_s = t_2 + \lambda_g/4 = z_{open}$ by a shorting plate, as shown in Fig. 3(a) (open-circuit method).

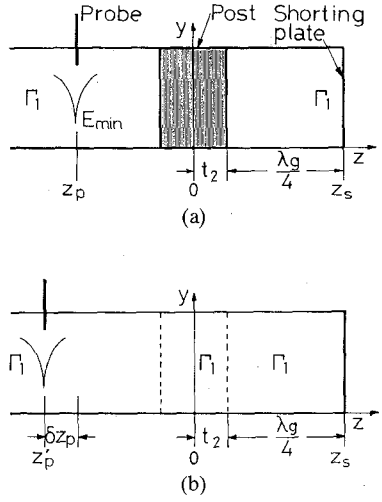

Fig. 3. Circuit diagram of the measurement of the reflection coefficients R_{open} (with a post) and R_{emp} (without a post) by the open-circuit method. The waveguide cell is terminated at $z = t_2 + \lambda_g/4 = z_{open}$ by a shorting plate, as shown in (a). $R_{open}(z_p)$ and $R_{emp}(z_p')$ are measured at the points $z = z_p$ in (a) and $z = z_p'$ in (b).

The distance $\lambda_g/4$ is long enough for the higher order mode to be attenuated. Measurement error due to the positioning error of a post for the open-circuit method is small compared with both the waveguide-matched termination method and the short-circuit method described in subsection C.

The reflection coefficient R_{open} for $z_s = z_{open}$ at $z = z_p$, where the voltage standing wave (VSW) has a minimum value and the voltage standing wave ratio (VSWR), S, is given by

$$R_{open}(z_p) = \left[P^- + \frac{U(1+P^+)^2}{1 - P^- U}\right]e^{2\Gamma_1 z_p} = \frac{1-S}{1+S}. \quad (25)$$

Here

$$U = qe^{-2\Gamma_1 z_{open}} = R_{emp}(z_p')e^{-2\Gamma_1 z_p'} = \frac{1-S'}{1+S'}e^{2\Gamma_1 z_p'} \quad (26)$$

where q is the reflection coefficient of the shorting plate (not equal to -1 due to its finite conductivity) and $\Gamma_1 = \alpha_c + [(\pi/a)^2 - k_0^2]^{1/2}$, where α_c is the attenuation constant of the empty waveguide. The change of the waveguide wall loss due to the insertion of a post is not negligible, because of the change of the distribution of current flowing in the waveguide wall due to the excitation of higher order modes in the neighborhood of the post. However, this effect is neglected here for simplicity. R_{emp} is the reflection coefficient without a post as shown in Fig. 3(b) at $z = z_p'$ where VSW has a minimum value and the VSWR is S'. We see that $z_p' = m\lambda_g/2 - \lambda_g/4 - t_2$, where m is the number of the VSW between $z = z_p'$ and $z = z_{open}$. From (25) and (26),

$$\frac{R_{open}(z_p)}{R_{emp}(z_p')}e^{-2\Gamma_1\delta z_p} = \frac{1}{U}\left[P^- + \frac{U(1+P^+)^2}{1-P^-U}\right] \quad (27)$$

where $\delta z_p = z_p' - z_p$ and is known directly from measurements. The complex conductivity can be obtained by using the iteration method for (27), as described in subsection C.

C. Calculation of Complex Conductivity

A computer program was developed to determine the complex conductivity of the post. The input parameters are measured values of δz_p, S (or $R_{\text{open}}(z_p)$), and S' (or $R_{\text{emp}}(z_p')$). The unknown parameters to be found are $\dot{\sigma}$ and c_1 or c_2. An optimum value of $\dot{\sigma}$ was obtained by the following two kinds of iteration methods:

1) The trial values are $\dot{\sigma}$ and c_1 or c_2. $P^{-\prime}$ and $P^{+\prime}$ in (24) are calculated with these trial values. An optimum value of $\dot{\sigma}$ for a trial value of c_1 or c_2 is calculated by the iteration method using the self-consistent equation for $\dot{\sigma}_n$ ($=\dot{\sigma}-i\omega\epsilon_0$) derived from (27) as

$$\dot{\sigma}_n^2 U(P^{+\prime 2}-P^{-\prime 2})+\dot{\sigma}_n(VU^2P^{-\prime}+2UP^{+\prime}+P^{-\prime}) + U(1-W)=0 \quad (28)$$

where $V=R_{\text{open}}(z_p)/R_{\text{emp}}(z_p')e^{-2\Gamma_1\delta z_p}$ and $W=[P^{-}+U(1+P^{+})^2/(1-P^{-}U)]/U$. Equation (28) is not a unique self-consistent equation to determine $\dot{\sigma}$. Optimum values of $\dot{\sigma}$ and c_1 or c_2 are found by searching matching points in the complex plane, where E_{int} must be equivalent to $E_{\text{inc}}+E_{\text{sct}}$ at $x=a/2\pm t_1$, $z=0$ or $x=a/2$, and $z=\pm t_2$ (boundary conditions (15)–(17)). This method is useful for thin posts, because $\dot{\sigma}_n$ does not converge to an optimum value for a thick post.

2) δz_p and $R_{\text{open}}(z_p)/R_{\text{emp}}(z_p')$ are obtained by measurements. While from (27), δz_p and $R_{\text{open}}(z_p)/R_{\text{emp}}(z_p')$ are given as

$$\delta z_p=-\frac{\text{Arg}(W)}{2\left[(\pi/a)^2-k_0^2\right]^{1/2}} \quad (29)$$

$$\frac{R_{\text{open}}(z_p)}{R_{\text{emp}}(z_p')}=|W|e^{2\alpha_c\delta z_p}. \quad (30)$$

Trial values are $\dot{\sigma}$ and c_1 or c_2. Their optimum values are found by searching matching points in the complex plane of $\dot{\sigma}$ so as to satisfy the boundary conditions given by (15)–(17), (29), and (30). This method is useful for thick posts, but is computationally slower than method 1) for lossy thin posts.

D. Measurement Error

The accuracy of the measured result of the complex conductivity is dependent on the accuracy of the basic formulation for $R(z)$ or $T(z)$, the positioning of the post in the waveguide, the VSWR measurement, the waveguide wall loss, and the shorting plate loss. In measuring a low conductivity, the waveguide wall loss and the shorting plate loss cause significant errors. The correction method of these errors is described above in subsection B. VSWR measurement is described in Section III.

Plots in Fig. 4(a) and (b) show calculated errors, $\Delta\sigma/\sigma$ and $\Delta\epsilon/\epsilon$, due to the deviation Δ of the position of a post from $z=0$ in the z direction, with $t_1/a=t_2/a=0.05$, $\sigma=0.001$ S/cm, and $\Delta=-0.01$ cm for the open-circuit method (OC), the waveguide-matched termination method (MT), and the short-circuit method (SC). $\Delta\sigma$ and $\Delta\epsilon$ indicate deviations from the true values of σ and ϵ for given values of Δ, respectively. Fig. 5(a) and (b) shows similar results for $\sigma=0.1$ S/cm and $\Delta=-0.01$ cm. The measurement error of the complex conductivity by OC is smaller than those for MT and SC. Fig. 6 shows the dependence of $\Delta\epsilon/\epsilon$ on post size $t_1/a(=t_2/a)$ for OC and MT for $\epsilon=2$ (SC is excluded because of the much larger values of the errors). A similar result was obtained for $\Delta\sigma/\sigma$. Measurement errors caused by the positioning

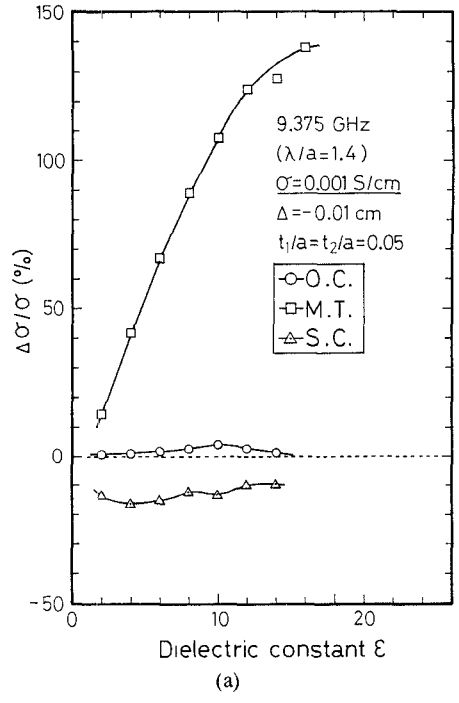

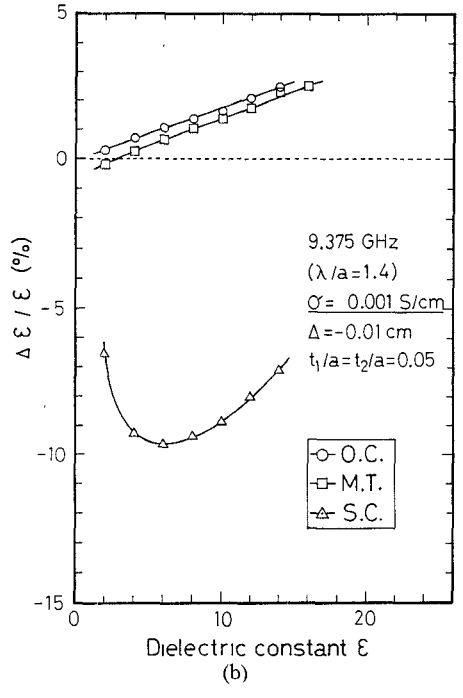

Fig. 4. Calculated values of (a) $\Delta\sigma/\sigma$ and (b) $\Delta\epsilon/\epsilon$ for $t_1/a=t_2/a=0.05$, $\sigma=0.001$ S/cm, and $\Delta=-0.01$ cm for the open-circuit method (OC), the matched termination method (MT), and the short-circuit method (SC).

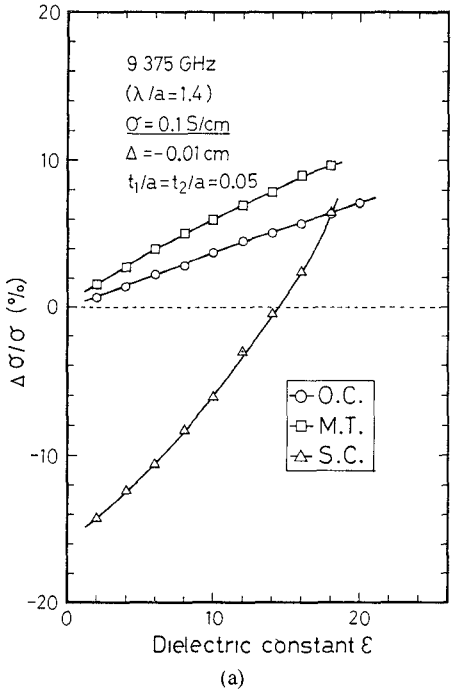

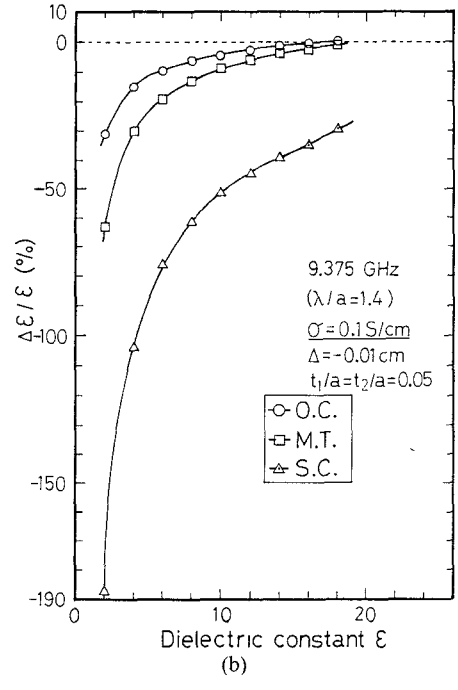

Fig. 5. Calculated values of (a) $\Delta\sigma/\sigma$ and (b) $\Delta\epsilon/\epsilon$ for $t_1/a = t_2/a = 0.05$, $\sigma = 0.1$ S/cm, and $\Delta = -0.01$ cm for various methods.

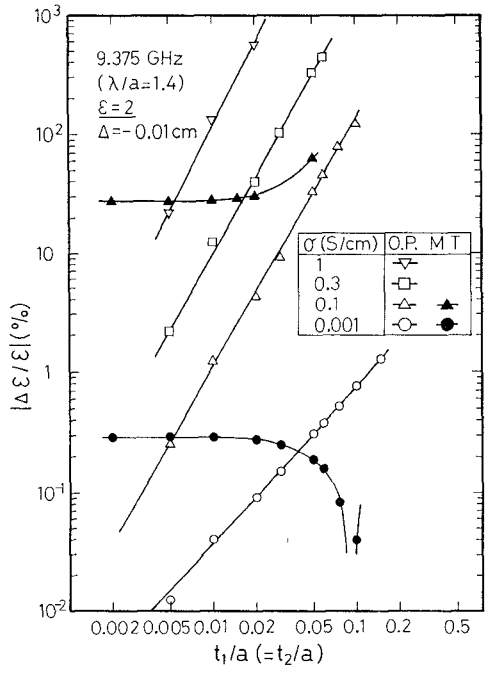

Fig. 6. Dependence of $\Delta\epsilon/\epsilon$ on the size $t_1/a(=t_2/a)$ of a post for various conductivities.

error increase with increasing post size for a given value of Δ. Therefore, the measurement error for the method using thin posts is smaller than the fully filled waveguide method. Measurement errors due to the deviation from $x = a/2$ in the x direction are small.

The solution of $R(z)$ in (22) or $T(z)$ in (23) is not valid for large posts having a high conductivity or dielectric constant. The validity of the basic formulation for $R(z)$ or $T(z)$ cannot be verified directly by the analytical method, because no rigorous solution for that is derived. However, the validity is verified roughly by checking not only the discrete boundary conditions given by (15)–(17), but also the continuous boundary conditions at the surface of a post, especially at the four corners of a post. The complex conductivity obtained on the basis of the above procedure was reasonable. A valid solution is obtained for $t_1 = a/2$, i.e., the fully filled waveguide method, because the boundary conditions at the four corners are satisfied.

III. Experimental

PTFE, synthetic quartz glass, sintered Al_2O_3 (99.5 percent), single crystals of rutile (parallel and perpendicular to the c axis), and n-type germanium were used as standard materials. PTFE, quartz glass, and sintered Al_2O_3 were selected because of the very low dielectric loss and low dielectric constants. Rutile was selected because of it high and widely varying dielectric constant with temperature and n-type germanium was selected because of its widely varying conductivity with temperature. Measurements were made at 9.375 GHz ($\lambda/a = 1.4$) using the open-circuit method. Standard waveguide WRJ10(WR90) with an inner width of $a = 2.29$ cm was used.

The standard values of the dielectric constants of PTFE, quartz glass, and Al_2O_3 at 9.375 GHz were obtained by the usual transmission line method with the cross section of the waveguide fully filled with a material [15]. They were 2.05 for PTFE, 3.80 for quartz glass, and 9.80 for Al_2O_3 (99.5 percent). The loss tangents $\tan\delta$ were 2×10^{-4} to 1×10^{-2}. The standard value of the static dielectric constant for rutile was obtained from the literature [16],

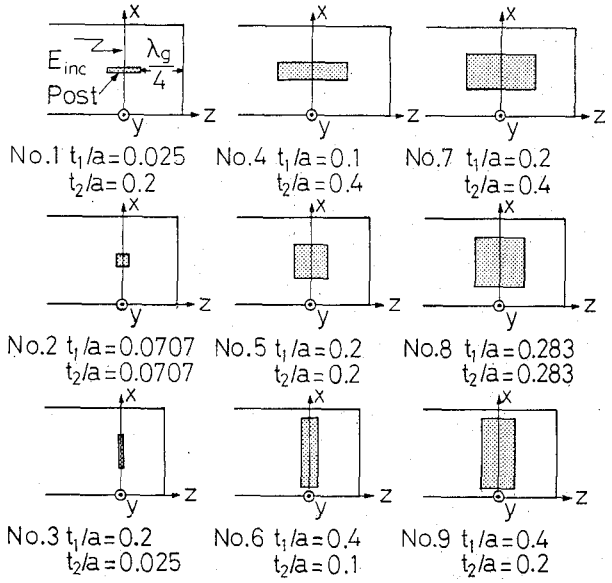

Fig. 7. Top views of waveguides loaded with posts with the various cross sections given in Table I.

[17]. The static dielectric constant is due to a soft, long-wavelength transverse-optic (TO) mode and is constant up to about 100 cm^{-1} [16]. The standard value of the conductivity for n-type germanium was obtained by the dc and ac (5 kHz) van der Pauw method [18]. Complex conductivities of a single crystal of $K_{1.6}Mg_{0.8}Ti_{7.2}O_{16}$ grown by a flux method were measured by impedance analyzers (YHP4192A and YHP4191A) from 100 Hz to 1 GHz and by the present method at 32.55 GHz to verify the accuracy of the conductivity measured at 9.375 GHz [12].

Each dielectric material was fitted to a rectangular waveguide by silver paste as shown in Fig. 1. For high-loss materials, good contact is necessary. Contact was checked by using two kinds of silver pastes. One was solidified at room temperature and the other was sintered at about 300°C. The same result was obtained. The probe displacement of the standing wave detector was measured by a dial gauge with an accuracy of 0.001 cm. The VSWR is calculated in terms of the probe displacement between points of twice the minimum height of the power standing wave measured by a small-signal rectifying diode with good square law verified by the precision resistance attenuator. Expansion or contraction of the waveguide due to a change of temperature was calibrated in advance of measurement.

IV. Results and Discussions

In this section, computed values of the complex conductivities or complex dielectric constants of the standard dielectric materials in terms of the iteration method described in Section III are presented. Computation of the reflection coefficient $R(0)$ or the complex conductivity $\dot{\sigma}$ required different times depending on the size and $\dot{\sigma}$ of the post. Computation of $R(0)$ for a post with $t_1/a = t_2/a = 0.05$ required about 2 s for $\sigma = 0$ S/cm and $\epsilon = 16.3$ (static dielectric constant of germanium) and 15 s for $\sigma = 1$ S/cm and $\epsilon = 16.3$ on a digital computer (HITAC M-280H), for example. Computation of $\dot{\sigma}$ from measured values of R_{open} and R_{emp} for the same size of post required about 60 s for $\sigma = 1$ S/cm and $\epsilon = 16.3$ on the same computer in terms of the method 1) described above in subsection II-C, for example.

A. PTFE, Quartz Glass, and Sintered Al_2O_3

Measured values of the reflection coefficient $R(0)$ and dielectric constants of PTFE, quartz glass, and sintered Al_2O_3 for the various cross-sectional sizes shown in Fig. 7 are shown in Table I and in Fig. 8 for a normalized cross-sectional area of $t_1t_2/a^2 = 0.04$ at 9.375 GHz. The dielectric constants agreed with the standard values. The results show that $R(0)$ for thin posts with low dielectric constants and the same area are almost the same for small values of the ratio of t_1/t_2 reported by Holms *et al.* [2]. This is not true for thicker or oblong posts with high dielectric constant. The solutions of $R(z)$ for dielectric materials with low dielectric constant and very low dielectric loss are reasonable over a wide range of values for t_1t_2/a^2 and the ratio t_1/t_2.

B. Single Crystals of Rutile

Fig. 9 shows the temperature dependences of the dielectric constants of single crystals of rutile in directions parallel and perpendicular to the c axis at 9.375 GHz. The cross-sectional sizes are $t_1/a = t_2/a = 0.025$ and $t_1/a = 0.024$, $t_2/a = 0.0245$, respectively. The boundary conditions at the four corners of the post are satisfied up to $\epsilon \sim 200$. The solid lines show values of the static dielectric constant of rutile obtained by Samara *et al.* [16] and Barrett [17] and agree with the measured values.

Plots in Fig. 10 show the dependences of measured values of $R(0)$ on the dielectric constants of rutile with a cross-sectional size of $t_1/a = t_2/a = 0.05$ in the direction perpendicular to the c axis. The solid lines show calculated values of the complex reflection coefficient for various dielectric constants. The solid lines do not agree with the measured values for rutile. Calculation shows that the resonance occurred at a dielectric constant of about 122 for this size. However, measurement showed that it occurred at a dielectric constant of about 88. This discrepancy is due to the unsatisfied boundary conditions at the four corners of the post; i.e., they are satisfied only up to $\epsilon \sim 40$ though the boundary conditions given by (15)–(17) are satisfied up to $\epsilon \sim 130$.

C. n-Type Germanium

Fig. 11(a) and (b) shows the temperature dependence of the conductivity and the dielectric constant of n-type germanium for various cross-sectional sizes. The dc conductivity is equivalent to the conductivity at 9.375 GHz between room temperature and 453 K [19]. The measured values of conductivity agree with those obtained by the van der Pauw method.

TABLE I
MEASURED REFLECTION COEFFICIENTS $R(0)$ AND DIELECTRIC CONSTANTS FOR VARIOUS CROSS-SECTIONAL SIZES OF PTFE, QUARTZ GLASS (QUARTZ), AND SINTERED Al_2O_3 CERAMICS AT 9.375 GHz

No.	Sample size			Reflection coefficient R(0) |R(0)| and Arg(R(0)) (deg)						Dielectric constant		
	t_1/a	t_2/a	S_n	PTFE		Quartz		Al_2O_3		PTFE	Quartz	Al_2O_3
1	0.025	0.2	0.005	0.124	262.9	0.332	250.6	0.484	216.5	2.01	3.72	9.81
2	0.0707	0.0707	0.005	0.121	262.7	0.353	249.3	0.795	214.6	2.01	3.88	9.76
3	0.2	0.025	0.005	0.115	263.3	0.335	250.5	0.698	225.0	2.04	3.74	9.65
4	0.1	0.4	0.04	0.0776	36.05	0.461	315.1	/	/	2.06	3.87	/
5	0.2	0.2	0.04	0.405	228.9	0.258	179.3	0.793	241.3	2.07	3.97	9.51
6	0.4	0.1	0.04	0.461	239.8	0.411	214.3	0.975	175.0	2.04	3.81	9.48
7	0.2	0.4	0.08	0.320	1.734	0.0369	255.7	/	/	2.06	3.89	/
8	0.283	0.283	0.08	0.0635	200.6	0.664	293.0	0.845	339.9	2.06	3.86	9.62
9	0.4	0.2	0.08	0.417	219.7	0.152	214.3	0.829	234.2	2.05	3.82	9.35

$S_n = t_1 t_2 / a^2$.
/: Solution not obtained.

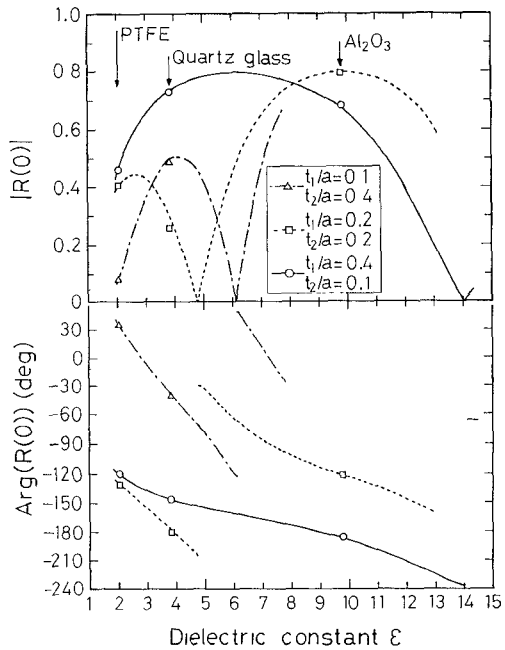

Fig 8. Measured values of the magnitude $|R(0)|$ and the phase angle $\mathrm{Arg}(R(0))$ of the reflection coefficients $R(0)$ of posts made of PTFE, quartz, and sintered Al_2O_3. The cross-sectional sizes are shown in Table I and Fig. 7. The solid lines show the calculated values of $R(0)$.

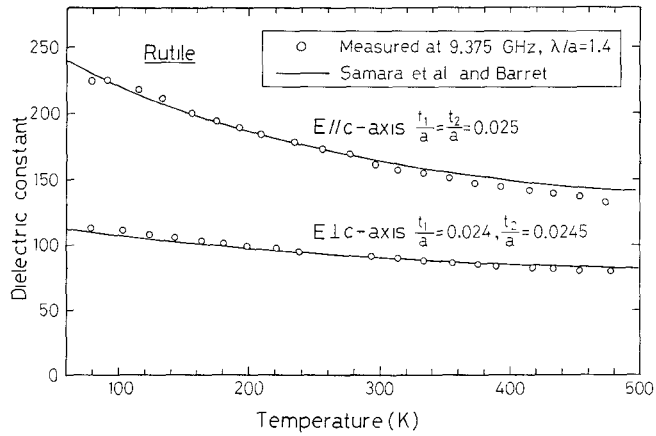

Fig. 9. The temperature dependences of the dielectric constants of rutile at 9.375 GHz. The cross-sectional sizes are $t_1/a = t_2/a = 0.025$ in the direction parallel to the c axis and $t_1/a = 0.024$ and $t_2/a = 0.0245$ in the direction perpendicular to the c axis. The solid lines show values of the static dielectric constants of rutile obtained by Samara *et al.* [16] and Barrett [17].

The solid line in Fig. 11(b) shows the temperature dependence of the dielectric constant below room temperature calculated by means of the classical model (Drude model) of conduction of electrons proposed by Benedict *et al.* with the conductivity effective mass of $0.12\,m_0$, where m_0 is the mass of a free electron, and the static dielectric constant of 16.3 in germanium [19], [20]. They agree with the measured values. Fig. 12 shows the temperature dependence of the dielectric constant of n-type germanium which completely fills the cross section of the waveguide calculated by the iteration method using the present

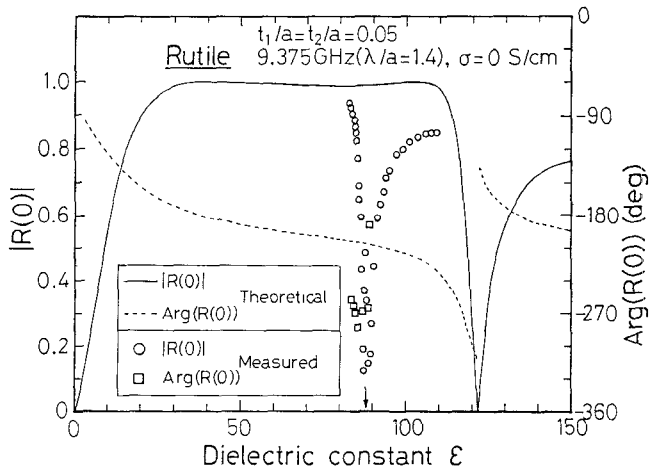

Fig. 10. The dielectric constant dependence of measured values of the reflection coefficient $R(0)$ of rutile in a direction perpendicular to the c axis for $t_1/a = t_2/a = 0.05$ at 9.375 GHz. The solid and broken lines show calculated values of the complex reflection coefficient.

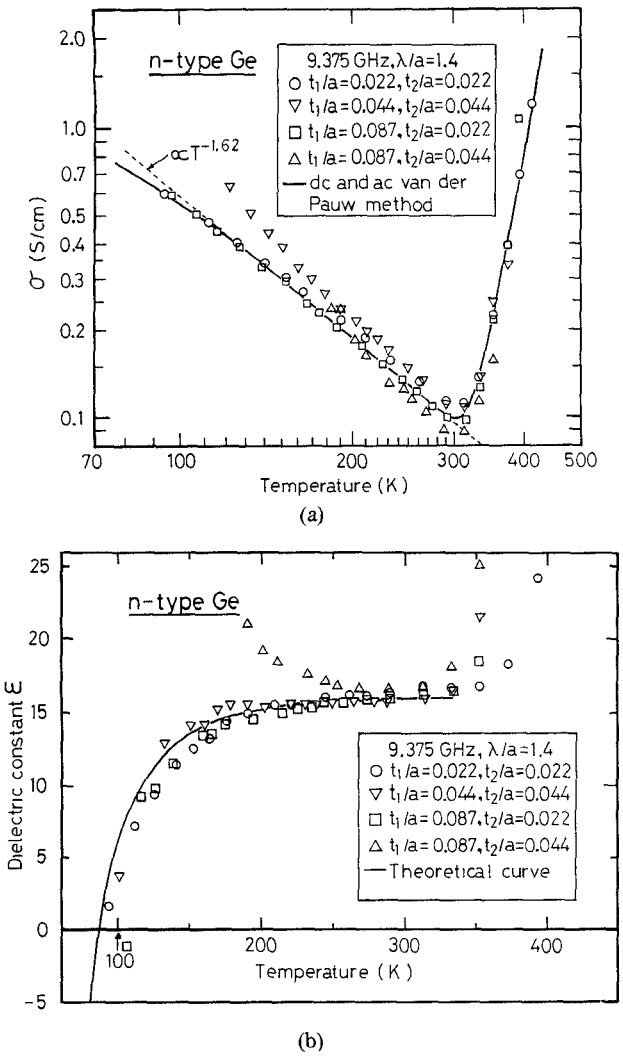

Fig. 11. Temperature dependence of (a) the conductivity and (b) the dielectric constant of n-type germanium with various cross-sectional sizes at 9.375 GHz. The solid line in (a) shows the values of conductivity measured by the dc and ac van der Pauw method and that in (b) shows the calculated values.

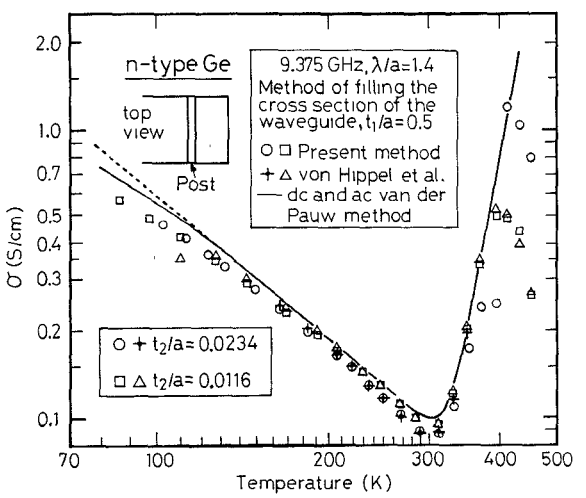

Fig. 12. The temperature dependence of the dielectric constant of n-type germanium, which completely fills the cross section of the waveguide, calculated by the present method and by the usual transmission line method [15].

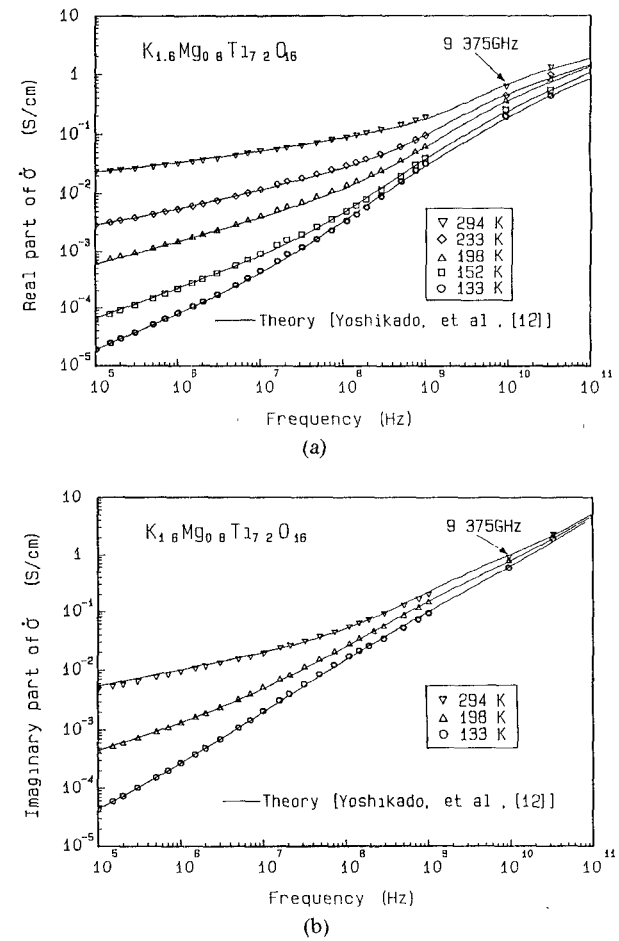

Fig. 13. Frequency and temperature dependences of the complex conductivity of potassium-magnesium-priderite, $K_{1.6}Mg_{0.8}Ti_{7.2}O_{16}$. The cross-sectional size is $t_1/a = t_2/a = 0.0039$. The solid lines show values calculated by the one-dimensional ionic conduction model [12].

method and the usual transmission line method [15]. Neither method gives a reasonable convergent solution for high conductivity and dielectric constant above room temperature for the thicker sample compared with the method using thin posts. This is mainly due to positioning error, as discussed in subsection II-D.

These results show that the method using posts gives a reasonable convergent value of the complex conductivity for a higher conductivity or dielectric constant for a thinner post of the lossy dielectric materials.

D. Priderites

Fig. 13(a) and (b) shows the frequency and temperature dependences of the complex conductivity of potassium-magnesium-priderite, $K_{1.6}Mg_{0.8}Ti_{7.2}O_{16}$. The cross-sectional size was $t_1/a = t_2/a = 0.0039$. Measured values at 9.375 GHz were consistent with values calculated by the one-dimensional ionic conduction model (shown in solid lines) [12].

V. Conclusions

A solution was derived for a scattered electric field from a square (oblong) lossy dielectric post in a rectangular waveguide. Then a simple formula for the reflection coeffi-

cient for a waveguide loaded with a square post was derived, and values of the complex conductivity of the post could be calculated by an iteration method. The accuracy of the derived solutions was verified by comparing measurement values with the values of the complex conductivity for standard materials whose values have been obtained by other measurement techniques and from the literature. Measurements were made by the open-circuit method, where the measurement error due to positioning of the post is comparatively small. Results show that the solutions are reasonable if the boundary conditions at the surface of the post in addition to the discrete boundary conditions are satisfied. They also are applicable to the method that involves completely filling the cross section of the waveguide. A method measuring the complex conductivity of the square dielectric post was established.

ACKNOWLEDGMENT

The authors wish to thank Dr. Fujiki, who is with the National Laboratory for Research in Inorganic Materials, for supplying single crystals of priderites.

REFERENCES

[1] N. Marcuvitz, *Waveguide Handbook*. New York: McGraw-Hill, 1951, pp. 257–271.

[2] D. A. Holmes, D. L. Feucht, and H. Jacobs, "Microwave interaction with a semiconductor post," *Solid-State Electron.*, vol. 7, pp. 267–271, Apr. 1964.

[3] T. Arizumi and M. Umeno, "Propagation characteristic in the waveguide loaded with a cylindrical semiconductor rod," *Trans. IECE Japan*, vol. 49, pp. 722–729, 1966.

[4] H. Ikegami, "Scattering of microwaves from a plasma column in rectangular waveguides," *Japan J. Appl. Phys.*, vol. 7, pp. 634–655, June 1968.

[5] E. D. Nielsen, "Scattering by a cylindrical post of complex permittivity in a waveguide," *IEEE Trans. Microwave Theory Tech.*, vol. MTT-17, pp. 148–153, Mar. 1969.

[6] N. Okamoto, I. Nishioka, an Y. Nakanishi, "Scattering by ferrimagnetic circular cylinder in a rectangular waveguide," *IEEE Trans. Microwave Theory Tech.*, vol. MTT-19, pp. 521–527, June 1971.

[7] G. Cicconi and C. Rosatelli, "Solutions of the vector wave equation for inhomogeneous dielectric cylinders in waveguide," *IEEE Trans. Microwave Theory Tech.*, vol. MTT-25, pp. 885–892, Mar. 1977.

[8] a) J. C. Araneta, M. E. Brodwin, and G. A. Kriegsmann, "High-temperature microwave characterization of dielectric rods," *IEEE Trans. Microwave Theory Tech.*, vol. MTT-32, pp. 1328–1335, Oct. 1984.
b) J. R. Dygas and M. E. Brodwin, "Frequency-dependent conductivity of NASICON ceramics in the microwave region," *Solid State Ionics*, vols. 18&19, pp. 981–986, 1982.

[9] H. Auda and R. F. Harrington, "Inductive post and diaphragms of arbitrary shape and number in a rectangular waveguide," *IEEE Trans. Microwave Theory Tech.*, vol. MTT-32, pp. 1328–1335, Oct. 1984.

[10] Y. Leviatan, D. Shau, and A. T. Adams, "Numerical study of the current distribution on a post in a rectangular waveguide," *IEEE Trans. Microwave Theory Tech.*, vol. MTT-32, pp. 1411–1415, Oct. 1984.

[11] K. Ise and M. Koshiba, "Numerical analysis of *H*-plane waveguide junction with dielectric posts by combination of finite and boundary elements," *IEEE Trans. Microwave Theory Tech.*, vol. MTT-34, pp. 103–109, Jan. 1986.

[12] S. Yoshikado, T. Ohachi, Y. Onoda, M. Watanabe, and Y. Fujiki, "ac ionic conductivity of hollandite type compounds from 100 Hz to 37.0 GHz," *Solid State Ionics*, vol. 7, pp. 335–344, 1982.

[13] R. E. Collin, *Field Theory of Guided Waves*. New York: McGraw-Hill, 1960, pp. 198–200.

[14] J. D. Kraus and K. R. Carver, *Electromagnetics*. New York: McGraw-Hill, 1973, pp. 363–425.

[15] A. R. von Hippel, *Dielectric Materials and Application*. New York: John Wiley, 1954, pp. 301–425.

[16] G. A. Samara and P. S. Peercy, "Pressure and temperature dependence of the static dielectric constants and Raman spectra of TiO_2 (rutile)," *Phys. Rev.*, vol. B7, pp. 1131–1148, 1973.

[17] J. H. Barrett, "Dielectric constant in perovskite type crystals," *Phys. Rev.*, vol. 86, pp. 118–120, 1952.

[18] L. J. van der Pauw, "A method of measuring the resistivity and Hall coefficient on lamellae of arbitrary shape," *Philips Tech. Rev.*, vol. 20, pp. 200–208, 1958.

[19] T. S. Benedict and W. Shockley, "Microwave observation of the collision frequency of electrons in germanium," *Phys. Rev.*, vol. 89, pp. 1152–1153, 1953.

[20] S. M. Sze, *Physics of Semiconductor Devices*. New York: John Wiley, 1981, pp. 27–30.

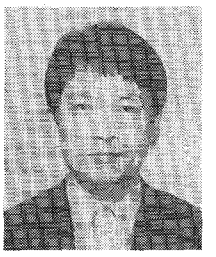

Shinzo Yoshikado was born in Osaka, Japan, on November 13, 1952. He received the B.S. degree in electrical engineering from Doshisha University, Kyoto, Japan, in 1976 and the M.S. degree in material science from the University of Electro-communications, Tokyo, Japan, in 1978.

In 1983, he joined the Department of Electrical Engineering, Doshisha University, where he is now an Assistant Professor. His research interests are in developing new superionic conductors and low-loss dielectric materials.

Ichiro Taniguchi received the B.S. degree in 1953 and the Ph.D. degree in 1961 in electrical engineering from Kyoto University, Kyoto, Japan.

In 1959, he joined the Department of Electronics, Doshisha University, where he is now a Professor of Electronics. His research interests are in semiconductor devices, microwave measurements, and plasma processing and diagnostics.